Available online at www.sciencedirect.com

SCIENCE DIRECT®

Structural Safety 28 (2006) 17–43

STRUCTURAL SAFETY

www.elsevier.com/locate/strusafe

Probabilistic finite element analysis using ANSYS

Stefan Reh [a,*], Jean-Daniel Beley [b], Siddhartha Mukherjee [b], Eng Hui Khor [b]

[a] *University of Applied Sciences, Berliner Tor 21, D-20099 Hamburg, Germany*
[b] *ANSYS Inc., 275 Technology Drive, Canonsburg, PA 15317, USA*

Available online 24 June 2005

Abstract

Driven by stiff competition, industrial manufacturers find themselves under growing pressure to optimize apparently conflicting technical and financial goals in an environment of ever increasing product complexity. In addition, this challenge is to be met under the existence of randomness and uncertainty, which the products are subjected to. Consequently, finding the right balance between conflicting goals under the existence of uncertainties requires the use of probabilistic tools. To achieve this, ANSYS Inc. has released two tools, namely the ANSYS Probabilistic Design System and the ANSYS DesignXplorer. This paper describes the problems that can be addressed, the underlying algorithms implemented and methodologies of these methods in both tools. A special topic of the paper is the discussion and explanation of the Variational Technology, which is offered in both tools. Variational Technology is a highly efficient method to provide accurate, high-order response surfaces based on a single finite element analysis. The capabilities, strengths and weaknesses of these methods are discussed. The possibility to reduce the execution time using parallel computing is discussed. Different measures to assess the accuracy and validity of the results obtained with the different probabilistic methods are given special attention. Various capabilities to post-process the probabilistic results are mentioned. The methods and the capabilities to optimize multiple and possibly conflicting goals are highlighted. Finally, the application of the software is illustrated using various industrial example problems.

Keywords: Uncertainty; Reliability; Design for Six Sigma; Reliability-based optimization; Robust design

* Corresponding author. Tel.: +49 40 42875 8715; fax: +49 40 42875 8799.
E-mail addresses: reh@rzbt.haw-hamburg.de (S. Reh), jean-daniel.beley@ansys.com (J.-D. Beley), siddhartha.mukherjee@ansys.com (S. Mukherjee), samuel.khor@ansys.com (E.H. Khor).

0167-4730/$ - see front matter
doi:10.1016/j.strusafe.2005.03.010

1. Introduction

Since quite a number of years, methods and tools to quantify the reliability and quality of mechanical products have received an ever-growing interest from industry as well as academia. Driven by the need to simultaneously reduce costs (manufacturing costs, warranty costs, etc.), reduce time-to-market, improve product quality and product reliability, industrial manufacturers find themselves challenged to optimize apparently conflicting technical and financial goals in an environment of ever increasing product complexity. In addition, this challenge is to be met under the existence of randomness and uncertainty, which the products are subjected to, since they are manufactured and operated under real-life conditions. Naturally, optimization is only possible if the optimization goals as well as possible constraints can be quantified. Consequently, finding the right balance between conflicting goals under the existence of uncertainties requires the use of probabilistic tools. In this context, the following analysis types are typically used to address this question:

Deterministic analysis. A deterministic analysis is the transformation function representing the relationship between the input variables influencing the behaviour of a product and the result parameters characterizing the product behaviour. In simple cases the result parameters can be expressed as an analytical function, but in realistic cases the input-output relationship is only given algorithmically for example using finite element program.

Uncertainty analysis. If the input variables influencing the behaviour of a product are uncertain, i.e. are subjected to scatter, then the primary task of an uncertainty analysis is to quantify how much the result parameters characterizing the product behaviour are affected by those uncertainties.

Reliability analysis. In order to quantify the reliability of a product it is useful to calculate the failure probability or non-conformance probability denoted with P_f. The reliability P_s is the probability that the product will survive or conforms to certain requirements, with $P_s = 1 - P_f$.

Reliability-based optimization. As the name implies, reliability-based optimization tries to optimize the reliability or failure probability. It should be noted, that improving the reliability often conflicts with other technical and financial goals. Hence, the optimization process should try to achieve a reasonable and quantifiable balance between all goals.

Robust design. Engineering products are becoming more and more complex and prone to the effects of uncertainty [1]. Robust design tries to optimize the design to make it less sensitive to unavoidable uncertainties, thereby reducing the variability in the product behaviour and making it more ‘predictable’. Achieving this is an optimization problem using the results of a probabilistic analysis as goals and constraint functions. Measures to quantify robustness (or the lack thereof) are for example the standard deviation or coefficient of variation, kurtosis, signal-to-noise ratios [2–4], Shannon’s entropy [5] or the failure probability of parameters describing the behaviour of a product.

Design for Six Sigma. The expression ‘Six Sigma’ was first devised by Motorola [6] defining that Six Sigma quality is given if only about 3.4 parts out of 1 million fall outside the limits given by the design requirements. In practice Design for Six Sigma is used either synonymously to robust design or to reliability-based optimization.

Multi-objective optimization. Improving the design of a product very often involves more than one goal. The more objectives are used to formulate the optimization problem then eventually some of them are conflicting, which means that improving one or more goals is only possible at the expense of one or more others.

Trade-off study. A trade-off study is a way to visualize conflicting goals in a multi-objective optimization in form of a Pareto front.

To address also the probabilistic analysis types mentioned above, ANSYS Inc. released two tools, namely the ANSYS Probabilistic Design System and the ANSYS DesignXplorer. Both tools can account for randomness in input variables such as material properties, boundary conditions, loads and geometry. Both tools can handle several of the analysis types mentioned above. In the following, the ANSYS Probabilistic Design System is referred to as '*the PDS*' and the ANSYS DesignXplorer is denoted as '*the DesignXplorer*'.

This paper describes these tools in terms of the problems that can be addressed, as well as their capabilities and limitations. The capabilities of the tools to characterize the probabilistic problem are outlined. A separate section is dedicated to the probabilistic methods and their underlying algorithms. Here, a special topic of the paper is the discussion and explanation of the Variational Technology, which is offered in both ANSYS tools. Variational Technology is a method to provide accurate, higher-order response surfaces based on a single finite element analysis. The capabilities, strengths and weaknesses of these methods are discussed. For each method the measures to assess the accuracy and validity of the results is given special attention. The computational effort associated with these methods is compared with each other and the possibility to reduce the overall computation time using parallel computing is mentioned. Various capabilities and methods to post-process the probabilistic results are discussed. Finally, the application of the software is illustrated using various example problems.

2. Probabilistic tools

To address the growing need for stochastic and probabilistic finite element analysis ANSYS Inc. released first version of the ANSYS Probabilistic Design System in the year 2000. In the meantime also the ANSYS DesignXplorer has been released, which is based on a user-friendly interface with easy access to parameters including CAD parameters. Both tools are addressing a different audience and have common as well as differing capabilities. The capabilities of both ANSYS tools are summarized in Table 1.

2.1. The ANSYS Probabilistic Design System

As the name implies, the ANSYS Probabilistic Design System (PDS) is made to address probabilistic problems. As such, it can be used for an uncertainty analysis or a reliability analysis. It is tightly integrated into ANSYS, using the same graphical user interface, hence having the same look and feel as ANSYS itself (see Fig. 1). The targeted audience is advanced engineers who are comfortable with performing finite element analyses using ANSYS on a regular basis. The PDS is based on the ANSYS Parametric Design Language (APDL), which allows users to parametrically build a finite element model, solve it, obtain results and extract characteristic results parameters such as the maximum stress for example. In addition, APDL

Table 1
Capabilities of the PDS and the DesignXplorer

Feature		PDS	DesignXplorer
Analysis types	Uncertainty analysis	Yes	Yes
	Reliability analysis	Yes	Yes
	Reliability-based optimization	No	Yes
	Robust design	No	Yes
	Design for Six Sigma	No	Yes
	Multi-objective optimization	No	Yes
	Trade-off study	No	Yes
Bi-directional, parametric associativity with CAD	DesignModeler	No	Yes
	SolidWorks	No	Yes
	SolidEdge	No	Yes
	Pro/ENGINEER	No	Yes
	Autodesk Inventor	No	Yes
	Mechanical Desktop	No	Yes
	Unigraphics NX	No	Yes
Mesh-based geometry variation with ParaMesh		Yes	2005+
Parallel, distributed computing	Unix-to-Unix	Yes	No
	Unix-to-PC	Yes	No
	PC-to-PC	Yes	2005+
	PC-to-UNIX	Yes	2005+
Operating system	Windows 2000/XP	Yes	Yes
	Solaris, SUN, HP	Yes	2005+
	AIX, Linux	Yes	No
Interface to other programs	NASTRAN	No	2005+
	ABAQUS®	No	2005+
	CFX™(CFD)	No	2005+
	Generic third party	No	2005+
	EXCEL™	No	2005+
Use expressions as result parameters		Yes	Yes
Price		Free	*

* For price information please contact the local sales representative.

provides the possibility to use input variables as well as result parameters in arithmetic expressions, do-loops and if-then-else constructs. As such the PDS is completely independent of the physics captured in a finite element analysis and for example covers the range from a typical linear elastic stress calculation to a more advanced coupled multi-physics analysis. Access to CAD parameters in ANSYS is problematic due to the fact that ANSYS lacks a bi-directional, parametric associativity to CAD systems. Access to geometry parameters in ANSYS is possible if either the geometry is defined with APDL or the finite element mesh is morphed to mimic a geometry variation. Mesh morphing can be done with a separate, stand-alone tool ANSYS ParaMesh.

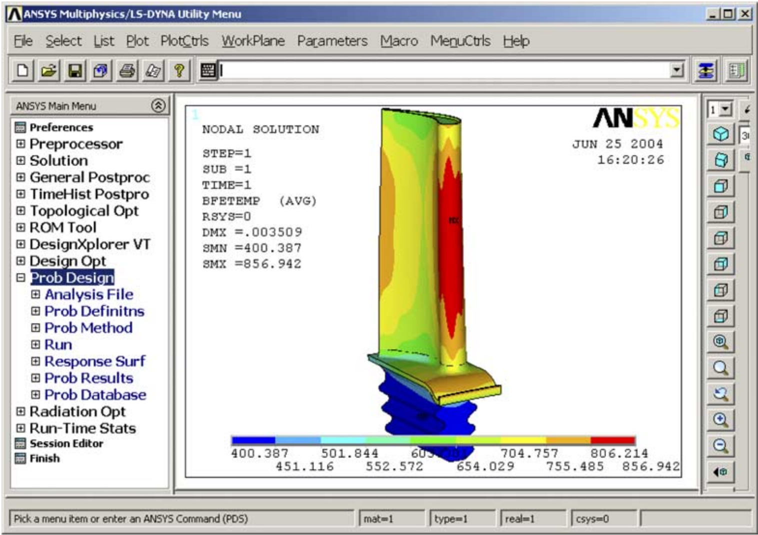

Fig. 1. The Probabilistic Design System integrated into ANSYS.

2.2. Advantages and disadvantages

The tight integration of the PDS into ANSYS plus the fact that the PDS comes with ANSYS at no extra cost is an advantage for ANSYS users. The PDS also includes the capability to distribute the necessary jobs in a heterogeneous network of computers, which drastically reduces the overall computation time. The PDS is a general-purpose probabilistic tool in the sense that it can utilize all deterministic analysis capabilities of ANSYS itself.

However, the tight integration into ANSYS also implies that the PDS cannot easily be coupled with other finite element packages. Handling of random geometry parameters may also be cumbersome in certain cases. This problem is better handled by the DesignXplorer, which is discussed next.

2.3. The ANSYS DesignXplorer

The ANSYS DesignXplorer is built on the new ANSYS object-oriented architecture, the ANSYS Workbench environment. The ANSYS Workbench provides access to the finite element capabilities of ANSYS in a very user-friendly and easy-to-learn fashion. In addition, users can add their own parameterized APDL commands to the analysis sequence, making all of the ANSYS finite element capabilities available for a probabilistic analysis using the DesignXplorer. In addition, the Workbench environment provides a set of functionalities to the applications that are built on this architecture, namely:

- *Parameter management.* Geometry, material properties, loads and boundary conditions as well as result quantities can be parameterized with just one mouse-click, as illustrated in Fig. 2. No manual interaction is required to assign new values to parameters, re-run the applications

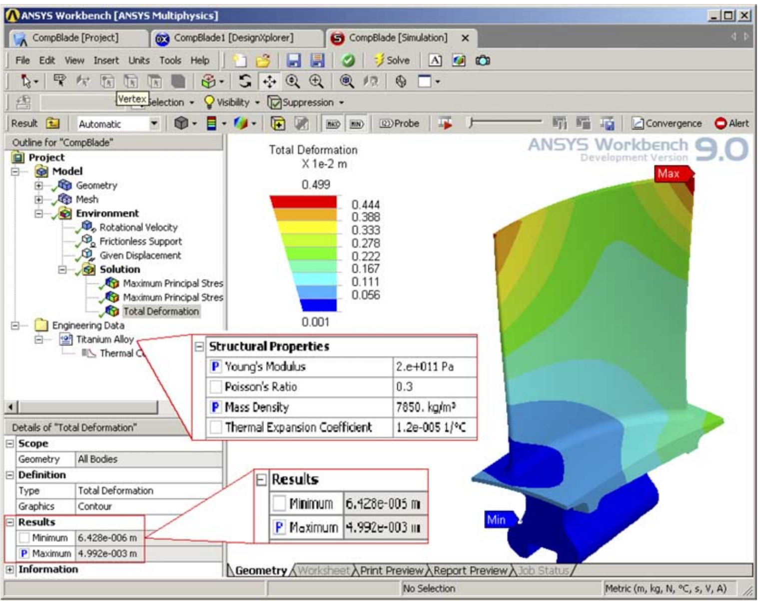

Fig. 2. Parameterization in the ANSYS Workbench environment (see the ‘P’ next to some input or result quantities).

affected by the parameter change and retrieving result parameters. In addition, the parameter management is sensitive to the physics of the parameter, e.g. if only a material property has changed its value, then automatically the steps to update the CAD model and re-meshing it are skipped.

- *Bi-directional, parametric associativity with CAD.* All loads and boundary conditions in a finite element analysis are consistently and automatically maintained, if for example a geometry parameter in the CAD model is changed.

The DesignXplorer automatically recognizes the parameters defined in the applications it is driving (see Fig. 3). The user can decide which parameters are design variables for optimization purposes and which ones are random variables. For the random variables the user can choose between several statistical distribution functions (see Section 3.). The DesignXplorer also allows the user to define derived result parameters in terms of analytic expressions of input and result parameters. The targeted audience for the DesignXplorer is designers and engineers who are more comfortable with an easy-to-use Windows based interface.

2.4. Advantages and disadvantages

The tight integration of the DesignXplorer into the ANSYS Workbench environment provides easy access to parameters, the bi-directional associativity with the CAD model and a user-friendly interface. Also, ANSYS Workbench environment will expand to include access to ABAQUS® and NASTRAN models (planned for 2005) and to include CFD capabilities (planned for 2005). This will automatically make the respective analysis capabilities available to the DesignXplorer, turning it into a more general-purpose probabilistic tool.

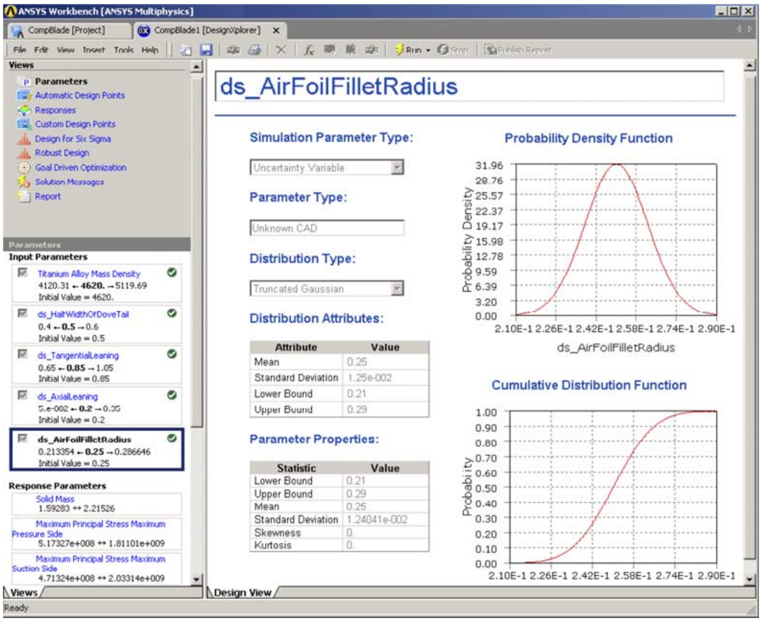

Fig. 3. The user-interface of the DesignXplorer.

At the moment the DesignXplorer does not allow Monte-Carlo simulation based on the finite element model. Also, it has no capability to distribute the finite element jobs in a network of computers. At the moment the DesignXplorer has no generic interface to third party applications. However, all these features are being worked on and are planned for release during 2005.

3. Characterizing the probabilistic model

In both ANSYS tools, the randomness of the input variables is characterized by the joint probability density function of the input variables [7]. Mixed moments of order higher than 2 are assumed to be negligible, which means that the joint probability density function can be described by the marginal distribution functions and the correlation structure.

Both ANSYS tools provide several statistical distribution functions to specify marginal distributions as listed in Table 2. The PDS allows the definition of correlation coefficients between random variables to characterize the correlation structure. To handle correlated random numbers the PDS uses the Nataf model as described by Liu and Der Kiureghian [8]. For the Nataf model the correlation coefficient between the arbitrarily distributed random variables must be transformed into the space of standard-normal distributed random variables by solving an integral equation. Liu and Der Kiureghian [8] suggested approximation functions to solve this integral equation for selected distribution types. In the PDS the integral equation is solved numerically, making the approach independent of the distribution type.

Neither the PDS nor the DesignXplorer can handle time dependent random effects in form of random processes. However, ANSYS has a tool to address Power Spectral Density (PSD) analysis based on Gaussian processes.

Table 2
Characterizing the probabilistic model in the PDS and the DesignXplorer

Feature		PDS	DesignXplorer
Distribution type	Normal (Gaussian)	Yes	Yes
	Truncated Gaussian	Yes	Yes
	Lognormal	Yes	Yes
	Uniform	Yes	Yes
	Triangular	Yes	Yes
	Exponential	Yes	Yes
	Gamma	Yes	Yes
	Weibull	Yes	Yes
	Beta	Yes	Yes
Correlated random variables		Yes	No
Random fields		Yes	No
Random processes		With PSD tool	No

4. Probabilistic methods

Both ANSYS tools offer several probabilistic methods. The PDS includes both the Monte-Carlo simulation method as well as response surface methods, while currently the DesignXplorer is based on response surface methods only. Both ANSYS tools allow the generation of response surfaces with traditional Design of Experiments as well as based on high-order derivatives using the Variational Technology. The probabilistic methods of both ANSYS tools are outlined in Table 3.

4.1. Monte-Carlo simulation methods

The fundamentals of the Monte-Carlo simulation method are well documented in literature [7,10] and shall not be repeated here. The key functionality of Monte-Carlo simulation techniques is the generation of random numbers with a uniform distribution from 0 to 1. The PDS uses the L'Ecuyer algorithm [11] for generating these random numbers, while the DesignXplorer uses the much more advanced Mersenne Twister algorithm [12]. Both ANSYS tools use the inverse probability method [7] to generate random numbers with arbitrary distributions. The implementation of the inverse cumulative probability function has been verified with the results published by Kececioglu [13] with matching results even for probabilities as low as 10^{-24}. Both ANSYS tools use the Latin-Hypercube sampling technique [14,15] to make the sampling process more efficient and to ensure that also the tails of the distribution of the input variables are better represented.

The interpretation of the results of a Monte-Carlo simulation analysis is based on statistical methods. The statistical procedures to calculate for example mean values, standard deviations and to derive histogram plots are available in textbooks on statistics and probabilistic methods, e.g. [16]. For the cumulative distribution function (CDF) the data is sorted in ascending order and the CDF of the ith data point, here denoted with F_i, can be derived from:

$$\sum_{k=i}^{N} \frac{N!}{(N-k)!k!} F_i^k (1-F_i)^{N-k} = 50\%. \tag{1}$$

In both ANSYS tools this equation is solved numerically for F_i. This implementation has been verified to exactly match the values given by Kececioglu [13]. From the CDF curve, failure probabilities as well as the inverse probability can be derived.

In ANSYS sensitivities are evaluated based on correlation coefficients [16]. The stronger a result parameter is correlated with a particular input variable, the more sensitive the result parameter is with respect to the input variable.

4.1.1. Accuracy and validity

Monte-Carlo simulation methods have only two major inaccuracies. Of course the number of samples cannot be infinite, but must be limited. The error due to the limitation of the number of samples can be easily quantified. As described in Ang and Tang [16], confidence intervals from statistical results of a Monte Carlo simulation can be easily obtained. In the context of finite element analyses another source of error, which is typically overlooked, is the error due to re-meshing the geometry if geometric uncertainties are included in the probabilistic model. Also minute changes in the geometry can cause the mesh density in critical areas of the geometry to change in a non-continuous fashion. This will lead to a change in the finite element results much larger than would be expected for a small geometry change. This error due to re-meshing cannot be easily quantified, but it can be minimized, if mesh controls are applied such as specifying the number of mesh divisions in critical areas of the geometry. But this is a manual and often time-consuming operation. The only method avoiding the influence of the meshing error is the Variational Technology, which will be explained later.

4.1.2. Advantages and disadvantages

The Monte-Carlo simulation method does not make any simplification or assumptions in the deterministic or probabilistic model. The only assumption it does in fact make is that the limited number of samples is representative to quantify the randomness of the result parameters. The error associated with this assumption is well quantifiable as outlined above. With increasing number of samples the Monte-Carlo simulation method converges to the true and correct probabilistic

Table 3
Probabilistic methods implemented in the PDS and the DesignXplorer

Feature		PDS	DesignXplorer
Monte-Carlo simulation	Direct (crude sampling)	Yes	No
	Latin-hypercube sampling	Yes	2005+
Design of experiment types	Box–Behnken design	Yes	No
	Central composite design	Yes	Yes
Versions of central composite designs	Face-centered	No	Yes
	Spherical	No	Yes
	Rotatable	Yes	Yes
	VIF optimized [9]	No	Yes
	User-defined α-value	No	Yes
Variational Technology		Yes	Yes
Monte-Carlo simulations on the response surface		Yes	Yes

result. The Monte-Carlo simulation is therefore widely used a the benchmark to verify the accuracy of other probabilistic methods. Another advantage is the fact that the required number of simulations is not a function of the number of input variables.

The disadvantage of the Monte-Carlo simulation method is its computational cost. As a rule of thumb, addressing low probabilities of failure requires about $N_{\mathrm{sim}} \approx 100/P_{\mathrm{f}}$ simulation loops, where P_{f} is the targeted failure probability. Hence, if the targeted failure probability is low, then the required number of samples may be prohibitively large, making the Monte-Carlo simulation method impractical for real engineering problems.

4.2. Response surface method

Response surface methods avoid the disadvantages of Monte-Carlo simulation methods by replacing the true input–output relationship by an approximation function. For the approximation function $\hat{y}$ typically a quadratic polynomial with cross-terms is used in the form:

$$\hat{y} = c_0 + \sum_{i=1}^{n} c_i \cdot x_i + \sum_{i=1}^{n} \sum_{j=i}^{n} c_{ij} \cdot x_i \cdot x_j. \tag{2}$$

Here, c_0, c_i and c_{ij} with $i,j = 1,\ldots,n$ are the regression coefficients and x_i, $i = 1,\ldots,n$ are the n input variables. Eq. (2) is also called the regression model.

4.2.1. Design of Experiments

Design of Experiments identify points in the space of input variables such that a response surface can be fitted in an accurate and efficient way. Two commonly used types of Design of Experiments are the Central Composite Design [3,17] and the Box-Behnken Design [18]. A Central Composite Design is composed of 2 axis points per input variable, the factorial points at the corners of the hypercube and one central point located at level. The Box-Behnken Design consists of one center point plus points located in the middle of edges of the hypercube.

In both ANSYS tools, the lower and upper levels of the input variables are determined by probabilities using the inverse cumulative distribution function. For example, by default the lower level corresponds to the 0.1% probability on the cumulative distribution function and the upper level corresponds to the 99.9% probability. Using probabilities for the lower and upper level of the Design of Experiment domain ensures that the domain always includes the same probability content, regardless of the distribution type of the input variables.[1]

For a Central Composite Design the number of factorial points goes up with the number of input variables n by 2^n, if a full factorial design is used. It is therefore necessary, to use a fractional factorial design [3,17]. It is beyond the scope of this paper to explain the fractional factorial designs and the role of the *resolution*. Suffice it to say that in both ANSYS tools the Central Composite Design is automatically generated such that the fractional factorial part always has a resolution of V (that is the roman numeral 5) or higher. Resolution V designs lead to the lowest number of factorial points, without impairing the accuracy and uniqueness of the regression coefficients in Eq. (2).

[1] We owe special thanks to Trevor Craney (formerly with Pratt&Whitney and now with Sikorsky), who provided invaluable input to our development efforts here.

It is noted, that the Box–Behnken design is limited in the number of input variables, with designs available only for cases with 3–7, 9–12 and 16 input variables. The Central Composite Design is more flexible, because designs are available for cases with 2–20 input variables. In addition, an investigation by Craney [9] compared the statistical properties of these two designs and identified the Central Composite Design as the better choice.

4.2.2. Regression analysis

The purpose of a regression analysis is to determine the regression coefficients. If $\underline{\hat{y}} = (\hat{y}_1, \ldots, \hat{y}_{N_{doe}})^{\mathrm{T}}$ is the vector of the approximated result values at the Design of Experiment points, then Eq. (2) can be written in matrix format:

$$\underline{\hat{y}} = \underline{\underline{D}} \cdot \underline{c}. \tag{3}$$

Here, $\underline{\underline{D}}$ is called the *Design Matrix* and $\underline{c}$ is the vector of regression coefficients. The element D_{ij} is the derivative of the approximation function (2) with respect to the jth regression coefficient at the location of the ith Design of Experiment point. Typically the method of least squares is used to determine the regression coefficients. For a linear regression analysis the regression coefficients are given by:

$$\underline{c} = \left(\underline{\underline{D}}^{\mathrm{T}}\underline{\underline{D}}\right)^{-1} \underline{\underline{D}}^{\mathrm{T}}\underline{y}. \tag{4}$$

4.2.3. Accuracy and validity

Response surface methods are based on the assumption that the response surface is an adequate representation of the true input–output relationship. It is also assumed that the residuals $(\underline{y} - \underline{\hat{y}})$ are normally distributed with constant variance. The goodness-of-fit measures implemented in both ANSYS tools to check the validity of those assumptions include the maximum variance inflation factor, the maximum leverage, the maximum absolute residual, the coefficient of determination, the p-value for normality, p-value of constant variance, the p-value for maximum studentized deleted residual to name just some of them [9,17,19]. Craney [9] has investigated those measures for real engineering applications and provided conditions for either rejecting or accepting a regression model. Also, the error associated with approximation function in Eq. (3) as well as its confidence intervals can be quantified as explained in [19]. Response surface methods are also affected by changes in the finite element mesh if geometry parameters are subjected to scatter. This is in fact true for almost all probabilistic methods based on finite element methods. As discussed for Monte-Carlo simulation methods, this error can be minimized. It can also be expected that the influence of this error is smaller compared to gradient based probabilistic methods, because the geometry changes applied during a Design of Experiment are larger than the Finite-Differences usually employed to evaluate gradients.

4.2.4. Improving the approximation

For engineering applications, a quadratic response surface according to Eq. (2) is often not sufficient to represent the true input-output relationship. To improve the accuracy of the approximation function, it is necessary to use non-linear transformation functions. This means that the result parameter y is first transformed according to $y^* = \psi(y)$ and then the transformed sample values y^*

are fitted with a quadratic response surface. The PDS uses the fixed transformation functions such as an exponential or logarithmic transformation as well as the Box–Cox transformation [20]. The DesignXplorer uses the Yeo–Johnson transformation [21]. In addition to the transformation of the result parameter the DesignXplorer also transforms the input variables. This is useful to cover cases, where the result parameter is for example a multiplicative function of the input variables.

In regression analyses, having more regression terms than needed, can lead to *overfitting*, which causes excessive variance in the regression coefficients. To further improve the regression model and avoid *overfitting* it is necessary to find out which regression terms are really important and should be included in the regression model and which ones are not. Both ANSYS tools use the forward-stepwise regression technique to select important terms [17,19].

4.2.5. Advantages and disadvantages

The advantage of response surface methods is obviously their performance. If the response surface is an adequate representation of the true input-output relationship, then the evaluation of the response surface is much faster than a finite element solution. Like Monte-Carlo methods, response surface methods are independent of the physics representing the true input-output relationship. All probabilistic methods other than Monte-Carlo simulation methods are based on a set of assumptions with respect to the deterministic or the probabilistic model. Therefore, another advantage of the response surface methods is that they inherently provide measures to verify, if the assumptions they are based on, are valid.

One of the disadvantages is that the response surface may be an inadequate representation of the true input–output relationship. This can happen for example, when the true input–output relationship is not continuous. However, this case is difficult to handle by any probabilistic approach other than Monte-Carlo methods. Another disadvantage is that the number of Design of Experiment points is strongly increasing with the number of input variables.

4.3. Variational Technology

In this section, the Variational Technology is described, as being an efficient and accurate alternative to Design of Experiments when applicable. The applicability of the Variational Technology depends on the analysis type and on the physical type of the parameters as listed in Table 4.

4.3.1. Background

Like Design of Experiments, the Variational Technology is also using a polynomial form for the response surface, but here the polynomial represents a Taylor expansion of the result parameter based on high-order derivatives at the center point of the variation range of the parameters. The derivatives are calculated during the solution of the finite element problem using Automatic Differentiation. If applicable, the Variational Technology largely increases the accuracy of the response surfaces as well as reduces the computational effort needed to obtain them.

4.3.2. Calculation of high-order derivatives

This section explains how to calculate the high-order derivatives of the solution with respect to the input variables. First, the derivatives of the finite element solution of a linear, static analysis are explained. Then the extension to a non-linear, static analysis and a modal analysis is given.

Table 4
Capabilities of the Variational Technology

Feature		ANSYS	DesignXplorer
Deterministic analysis type	Structural	Yes	Yes
	Normal modes	Yes	Yes
	Buckling	Yes	Yes
	Thermal	2005+	2005+
Parameter type	Boolean (set of elements)	Yes	Yes
	Material parameters	Yes	Yes
	Lumped mass	Yes	No
	Excitation frequency	Yes	No
	Shell thickness	Yes	Yes
	Layer thickness in shells	Yes	No
	Body temperature	Yes	No
	CAD geometry	No	Yes
	Geometry using ParaMesh	Yes	Yes

4.3.2.1. High-order derivatives for a linear, static analysis. The static equilibrium of a structure by the finite element method is considered. The displacement field U is solution of the linear system:

$$K(p_0)U(p_0) = F(p_0), \tag{5}$$

where stiffness matrix K and the load vector F are formed for a given parameter set p_0, defined from the geometry, material properties, loads and boundary conditions. Because the relation between p_0 and U is non-explicit, the usual way to get the displacement for another parameter set $U(p_1)$ is to solve Eq. (5) again.

Even when U is a non smooth vector, for e.g., close to a geometrical singularity such as a crack, U is analytical as long as K and F are analytical. Hence, U is identically equal to its Taylor expansion inside its convergence domain.

The first order derivatives of Eq. (5) are commonly used in structural optimization. Haftka [22] introduces the second order derivatives. The derivative of Eq. (5) with respect to p at $p = p_0$ up to an arbitrary order n is given by:

$$KU^{(n)} = F^{(n)} - \sum_{i=1}^{n} \binom{n}{i} K^{(i)} U^{(n-i)}. \tag{6}$$

The decomposition of the K matrix is already available from the solution of Eq. (5). Therefore, the derivatives of the displacement field expressed in Eq. (6) can be calculated with a small computational effort, once the right hand side of Eq. (6) has been formed, i.e. once the high order derivatives of the stiffness matrix and force vector have been calculated. These quantities can be obtained from the assembly of the elementary matrices and vectors:

$$K^{(i)} = \sum_{k \in \kappa} K_{el}^{(i)}.$$

Using a numerical integration, K_{el} is expressed as a sum over the integration points:

$$K_{\mathrm{el}} = \sum_{p} \omega_p (B_p^{\mathrm{T}} D_p B_p \det(J_p)),$$

where B is the strain/displacement matrix, D is the Hooke matrix, J_p is the determinant of the Jacobian matrix. Using the same integration scheme, the i^{th} derivative of the elementary stiffness matrix takes the form:

$$K_{\mathrm{el}}^{(i)} = \sum_p \omega_p (B_p^{\mathrm{T}} D_p B_p \det(J_p))^{(i)}.$$

Applying the Leibniz formula, i^{th} derivative of the product $(B_p^{\mathrm{T}} D_p B_p \det(J_p))$ becomes a product of the i^{th} derivatives of B, and $\det(J)$, as a function of the nodal coordinates of the element and derivatives, and D, as a function of the material properties of the element.

As the Taylor expansion of the matrix calculation is built on the same mesh as for the initial solve, the discretization error of the Taylor expansion term is also the same as for the initial solve. To get the derivatives of B, D, and $\det(J)$, an efficient approach is to use Automatic Differentiation, as shown in by Guillaume [23] and Beley et al. [24]. Guillaume [23] demonstrates that the derivatives calculated that way have the same binary representation as the exact derivatives.

4.3.2.2. High-order derivatives for a non-linear, static analysis. Let us consider now the displacement field U, being solution of a non-linear equation:

$$F(U(p_0), p_0) = 0, \tag{7}$$

where F is the residual force vector. For $p = p_0$, let us denote U^* the solution of Eq. (7).

The first derivative of U with respect to p, $U^{(1)}$, for $p = p_0$ and $U = U^*$, is obtained from Eq. (7):

$$\frac{\mathrm{d}F}{\mathrm{d}U} U^{(1)} = -\frac{\partial F}{\partial p}. \tag{8}$$

The $\frac{\mathrm{d}F}{\mathrm{d}U}$ is the usual iteration matrix. This matrix is formed and decomposed to reach the convergence of Eq. (7). The system Eq. (8) becomes a linear system, very similar to Eq. (5).

The second derivative of U with respect to p, $U^{(2)}$, and the high order derivatives $U^{(n)}$ are obtained from Eq. (8):

$$\frac{\mathrm{d}F}{\mathrm{d}U} U^{(n)} = \left(\frac{\partial F}{\partial p}\right)^{(n-1)} - \sum_{i=1}^{n-1} \binom{n-1}{i} \left(\frac{\mathrm{d}F}{\mathrm{d}U}\right)^{(i)} U^{(n-i)}.$$

The computational cost to obtain these derivatives is similar to the cost to calculate the derivatives of a linear displacement field and much smaller than the cost to get the initial solution of Eq. (7). This method has been applied in nonlinear mechanics (large displacements, nonlinear visco-elastic behavior law), CFD [25], and electromagnetism with nonlinear material behavior laws [26].

4.3.2.3. High-order derivatives for a modal analysis. Let us consider (λ,ϕ), solution of:

$$(K - \lambda M)\phi = 0, \tag{9}$$

where M is the mass matrix. To fully define ϕ, one adds an additional normalization equation:

$$\phi^{\mathrm{T}} M \phi = 1. \tag{10}$$

Derivatives of the eigenvalue problem. The first derivatives of eigenvalue problems are due to Rogers [27], Nelson [28], and later by Ojalvo [29]. The system formed by Eqs. (9) and (10) is a non-linear system, and needs to be derivated once similarly to Eq. (8) to form a system in λ' and ϕ':

$$\begin{aligned} &K\phi' - \lambda M\phi' - \lambda' M\phi = -K'\phi + \lambda M'\phi, \\ &\phi^{\mathrm{T}} M\phi' = -\frac{1}{2}\phi^{\mathrm{T}} M'\phi. \end{aligned} \tag{11}$$

Introducing the following notation:

$$\begin{aligned} S_\phi^{(n)} = &-\sum_{i=0}^{n}\binom{n}{i}(i+1)K^{(i+1)}\phi^{(n-i)} + \sum_{i=0}^{n}\binom{n}{i}\lambda^{(n-i)}\left(\sum_{j=0}^{i}\binom{i}{j}(j+1)M^{(j+1)}\phi^{(i-j)}\right) \\ &-\sum_{i=1}^{n}\binom{n}{i}(n-i+1)K^{(i)}\phi^{(n-i+1)} + \lambda\sum_{i=1}^{n}\binom{n}{i}(n-i+1)M^{(i)}\phi^{(n-i+1)} \\ &+\sum_{i=1}^{n}\binom{n}{i}\lambda^{(i)}\left(\sum_{j=0}^{(n-i)}\binom{n-i}{j}(n-i-j+1)M^{(j)}\phi^{(n-i-j+1)}\right) \\ &+\sum_{i=1}^{n}\binom{n}{i}(n-i+1)\lambda^{(n-i+1)}\left(\sum_{j=0}^{i}\binom{i}{j}M^{(j)}\phi^{(i-j)}\right) \end{aligned}$$

the high order derivatives of the mode shape can be expressed as:

$$(n+1)K\phi^{(n+1)} - (n+1)\lambda M\phi^{(n+1)} = S_\phi^{(n)} + (n+1)\lambda^{(n+1)}M\phi. \tag{12}$$

By definition, one has $(K - \lambda M)\phi = 0$. Consequently:

$$(n+1)K(\phi^{(n+1)} + \alpha\phi) - (n+1)\lambda M(\phi^{(n+1)} + \alpha\phi) = S_\phi^{(n)} + (n+1)\lambda^{(n+1)}M\phi \quad \forall\alpha. \tag{13}$$

Thus, the system in Eq. (12) is singular. Decomposing the derivatives of the modal shape over a reduced reference modal basis $(\widetilde{\Phi}, \widetilde{\Lambda})$ of m eigenfrequencies and vectors leads to the following expression:

$$\widetilde{\Lambda}v - \lambda v = \frac{1}{(n+1)}\widetilde{\Phi}^{\mathrm{T}}\left(S_\phi^{(n)} + (n+1)M\phi\lambda^{(n+1)}\right). \tag{14}$$

This system is diagonal, and is solved explicitly. However, from Eq. (13), this system has the singularity for $\widetilde{\Lambda}_i = \lambda_i$. The coefficient v_i can be chosen arbitrarily. One can for example use the normalization in Eq. (10) on the sum of the Taylor expansion, i.e., the updated mode shape.

4.3.3. Parameters

The equations in the previous sections have been derived using a formal parameter p. Every quantity that is used to form the stiffness and mass matrices or the load vector can be a parameter for the analysis. Typical parameters of a finite element model are material properties, physical properties such as the thickness of a shell element or the mass value of a lumped mass element, but the Variational Technology also handles less common parameters, such as CAD or mesh-based shape parameters and Boolean parameters.

Geometry parameters. The Variational Technology is based on Taylor Expansions. That implies that the variation with respect to the parameters has to be differentiable. Shape variations are usually handled using re-meshing. Re-meshing is most of the time a non-differentiable process, i.e., a geometry parameter changes can lead to a different number of nodes and elements. Mesh perturbation, i.e., modification of the location of the nodes of the mesh, is an alternative to re-meshing, which is differentiable. Building the mesh perturbation can be done automatically using the ANSYS Workbench parametric CAD plug-in, or be purely mesh based, using ANSYS ParaMesh.

Boolean parameters. Boolean parameters correspond to sets of elements in the model that can be turned ON or OFF. Internally, a continuous scaling parameter α acting on the stiffness and mass element matrices is introduced. The internal α parameter can be evaluated only for two values: 1 corresponds to the set of elements being active, 0 corresponds to the set of elements being inactive. These Boolean parameters can be used to study presence or absence of spot welds, bolts, holes, and so on.

4.3.4. Accuracy and validity

As shown in Section 4.3 calculating high-order derivatives of the results of a finite element analysis is possible with only one finite element solution. However, it still needs to be addressed whether or not the approximation of the output variation based on the high-order derivatives is a valid approximation and if it is valid, which derivation order shall be used. To answer these questions, a simple example of a spring having a spring stiffness k and a lumped mass m under gravity load is considered as shown on the left side of Fig. 4. The equation to determine the extension u of the spring under load given by $ku = -mg$. Introducing a parameter p to vary the spring stiffness in the form of $k(1 + p)$, the exact solution for the displacement u is given by $u = \frac{-mg}{k(1+p)}$. After building the Taylor expansion of u with respect to p at $p = 0$, we can plot the difference between the exact solution u and the sum of the Taylor expansion as a function of the parameter p value for various derivation orders as shown in the right side of Fig. 4. As expected the error is decreasing with the derivation order, but the error is always large for

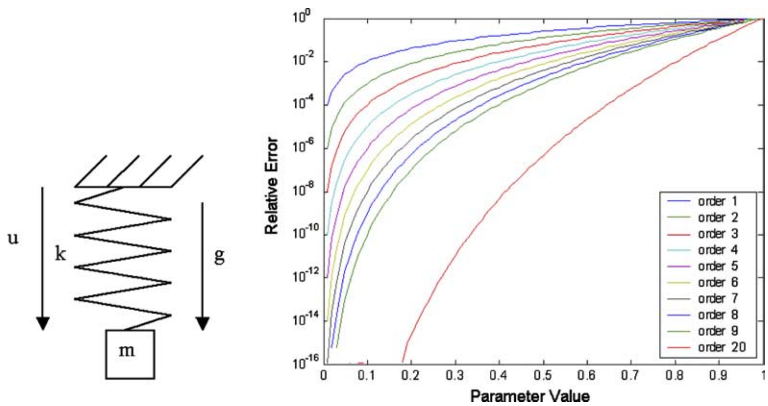

Fig. 4. Mass spring example (left) and its solution error (right).

values of p close to 1. The value $p = -1$ is a pole of the Taylor expansion, as the system's stiffness $k(1 + p)$ will be equal to 0. Therefore, also values of p close to 1 are close to the convergence radius of the Taylor expansion. By extension, every parameter value p in Eq. (5) such that $det(K(p)) = 0$ will be a pole of the Taylor expansion. The poles can correspond to physical properties singularities for example a shell element thickness equal to 0 or be geometrical singularities. By determining the poles, the valid range of the Taylor expansion can be found, as well as the appropriate derivation order.

4.3.5. Improving the approximation

When the center value of the parameters is too close to a singularity, building a polynomial approximation based on the Taylor expansion is not very efficient. It requires a large number of terms, and cannot approach the singular value of the parameter. In that case, using the high order derivatives of the solution at the center value, other approximation functions – such as the Padé approximation – can be built. More details on how to build a Padé approximation from the derivatives can be found in [30].

4.3.6. Advantages and disadvantages

The obvious advantage of the Variational Technology is its computational efficiency. Also, the Variational Technology builds an error estimator as a continuous function of the input parameter values. From this, the accuracy of the approximation can be guaranteed for the entire variation domain of the input variables. Due to high-order of the derivates used in the approximation function it is possible to accurately cover a wide range of the input variables. Another factor increasing the accuracy Taylor expansion is the fact that it is built for all the Finite Element results. Quite often result parameters are defined as spatial extrema of finite element results, for example the maximum stress or the maximum deflection in the finite element model. These extrema are likely to change location as the input variables are changing values. This leads to non-smooth response surfaces, even if the local stresses or deflections are smooth. As mentioned above, the mesh error adversely affected probabilistic results if geometry parameters are involved. The Variational Technology avoids re-meshing and is therefore insensitive to the mesh configuration. Using the same mesh for all shape variations, the Variational Technology can provide an accurate input-output relationship even for non-converged meshes.

The Variational Technology is of course not as generally applicable as for example Design of Experiments. Naturally, the implementation of the derivatives depends on the physical type of the input variable, the physical type of the result parameter and the analysis type, i.e. the underlying differential equation. Extending the applicability of the Variational Technology in all three directions, i.e. to cover more types of input variables, result parameter and analysis types is a committed long-term goal.

5. Probabilistic post-processing

Both ANSYS tools provide several ways to quantify and visualize probabilistic results. Basic statistical properties such mean values, standard deviation, skewness, kurtosis of result parameters and many others are provided to understand and quantify the variability of result parameter.

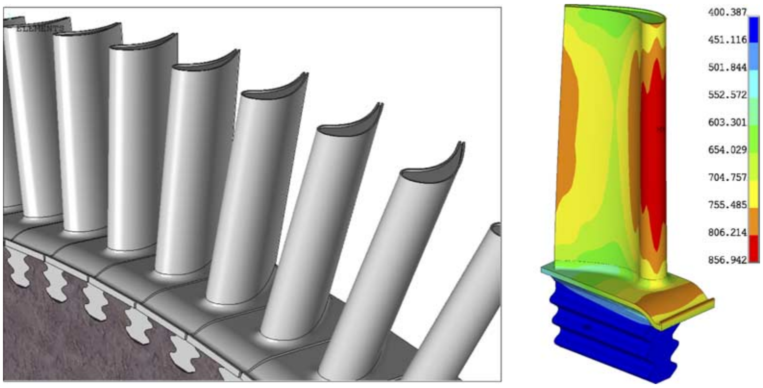

Fig. 5. Geometry of the turbine stage (left) and blade temperatures (right).

Histogram plots and cumulative distribution function (CDF) plots help to visualize the scatter of a result parameters and to quantify probabilities. To better visualize the tails of the distribution the CDF can be visualized in form of a Gauss plot, a Lognormal plot or a Weibull plot. Sensitivities provide vital information to improve the design towards higher reliability and quality. If the failure probability is too high, the most important input variables should be addressed to see if they can be used to lower the failure probability. Obviously, trying to improve the reliability of a product by focusing on insignificant input variables is not meaningful. The information about the insignificant input variables can also be very useful. If the design is already reliable enough, then there is usually the desire to reduce the cost of manufacturing without sacrificing reliability. In this case it is possible to loosen manufacturing tolerances for insignificant geometry parameters, because widening the tolerances will not affect the reliability. However, in this case it is recommended to repeat the probabilistic analysis using the new tolerance settings. A patented technology[2] is used to automatically generate a web-enabled report describing the probabilistic model, the probabilistic methods and the probabilistic results.

6. Application examples

6.1. Reliability analysis of a turbine stage

6.1.1. Deterministic model and results

The application example is a probabilistic analysis of the lifetime of a turbine stage with 100 blades mounted on a disk, as illustrated in Fig. 5. This example shows the capabilities of the PDS to address reliability problems. The geometry of the blades was built in ANSYS. All material properties as well as thermal and static boundary conditions are arbitrary numbers, but represent realistic scenarios. The deterministic model includes a thermo-mechanical analysis of a turbine blade plus a post-processing step to address various lifetime parameters. The blade is exposed

[2] US patent 6,055,541.

to a hotgas on the outside and cooled from the inside leading to a complex temperature field as illustrated in Fig. 5. In addition, the blades are subjected to centrifugal loads causing high stresses at the root of the airfoil. One finite element analysis of the blade plus the lifetime calculations took about 2.5 h to complete. The turbine blade is subjected to several failure modes. The ON and OFF cycles of the machine cause thermo-mechanical fatigue to the turbine blades, which is most severe at locations where temperatures are highest (see Fig. 5). The fatigue lifetime is determined using a known function between the LCF lifetime and the metal temperature and the stress at any given node. The machine running at elevated temperatures is exposing the blade leading edge to oxidation, which is causing a depletion of the oxidation protection coating. The oxidation lifetime is calculated by the time it takes until the accumulated depletion is equal to the thickness of the oxidation protection coating, assuming that the oxidation resistance of the base material is negligible. The machine running at elevated temperatures is causing creep deformations in the blade, leading to creep failure in the root cross-section of the airfoil. The creep lifetime is determined using a known function between creep lifetime and the average cross-sectional stress and temperature.

6.1.2. Description of the probabilistic model

The turbine blade is manufactured in a casting process. Imperfections in the casting process cause the core making up the inner cooling cavity to shift. Also the process of applying the oxidation protection coating has uncertainties leading to variability in the resulting thickness of the coating. All characteristic material properties, strength parameters and thermal boundary conditions of the turbine blade are considered as random variables as well, leading to a total of 17 random input variables for a blade. Table 5 summarizes the random input variables and their distribution. Here, 'NORM' and 'LOGN' denote the normal and the log-normal distribution respectively, both with mean value and standard deviation as distribution parameters and 'UNIF'

Table 5
Random input variables for the turbine blade

Type	Input variable	Distribution
Blade geometry	Tangential core shift (mm)	UNIF(−0.6, +0.6)
	Axial core shift (mm)	UNIF(−0.6, +0.6)
	Oxidation prot. coating thickness (mm)	LOGN (0.3, 0.03)
Blade material	Young's modulus (*)	NORM(1.0, 0.04)
	Density (kg/m^3)	NORM(8440, 422)
	Coefficient of thermal expansion (*)	NORM(1.0, 0.05)
	Heat conduction (*)	NORM(1.0, 0.05)
	Heat capacity (*)	NORM(1.0, 0.04)
	Oxidation depletion rate of coating (*)	LOGN(1.0, 0.05)
	Low cycle fatigue strength S/N-curve (*)	LOGN(1.0, 0.15)
	Creep rupture strength (*)	LOGN(1.0, 0.10)
Blade thermal boundary conditions	Hotgas temperature shift (°C)	NORM(0.0, 25.0)
	Hotgas heat transfer coefficient (*)	LOGN(1.0, 0.2)
	Hotgas mass flow (*)	NORM(1.0, 0.03)
	Cooling air temperature shift [°C]	NORM(0.0, 10.0)
	Cooling air heat transfer coefficient (*)	LOGN(1.0, 0.1)
	Cooling air mass flow (*)	NORM(1.0, 0.05)

is the uniform distribution characterized by the lower and upper bounds. The random variables indicated with (*) are random factors applied to quantities that are functions of temperature or location. For example, as suggested by Reh et al. [31,32], the randomness of the heat transfer coefficient h is modeled as $h_{\mathrm{rand}}(x,y,z) = C_{\mathrm{h}} \cdot C_{\mathrm{m}}^{0.8} \cdot h_{\mathrm{nom}}(x,y,z)$, where C_{h} is the random factor covering the uncertainty in the heat transfer mechanism itself and C_{m} is the random factor covering the uncertainty in mass flow and h_{nom} is the nominal heat transfer coefficient at the same x, y and z location.

6.1.3. Probabilistic results

The reliability of the blade was calculated with two different probabilistic methods implemented in the PDS, namely the Monte-Carlo simulation method and the response surface method. For the Monte-Carlo simulation, 500 samples have been performed. The response surface method required 291 Design of Experiment runs plus 10,000 Monte-Carlo runs exploiting the response surfaces. The 10,000 Monte-Carlo runs on the response surfaces took only about 4 seconds to complete, which illustrates the computational advantage of the response surface method. Fig. 6 shows the cumulative distribution function for the individual failure modes. It is noted that due to the limited number of samples the Monte-Carlo results are only accurate in a probability range from 2% to 98%. It is obvious from Fig. 6 that in this range, the results of the response surface method adequately match the Monte-Carlo results. It also can be concluded that oxidation of a blade is not likely failure mode, because a blade will more likely fail due to fatigue or creep rupture.

Also shown in Fig. 6 are the sensitivities of the low cycle fatigue failure mode of the blade with respect to the random input variables. As explained in Section 5, these sensitivities can be used to efficiently improve the design towards a higher reliability or to find out which tolerances can be relaxed to save manufacturing costs without sacrificing reliability. In this example, it is interesting to point out, that in a traditional deterministic analysis the scatter of the SN-curve representing the low cycle fatigue strength is the only input variable covered by statistical methods for example by using 99% exceedence values. The randomness of most other input variables considered here is

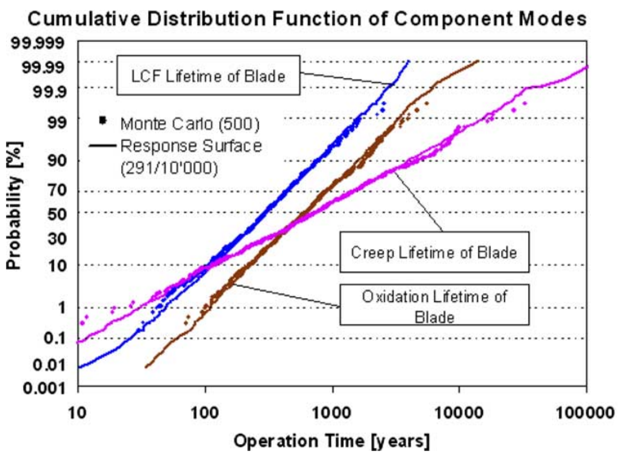

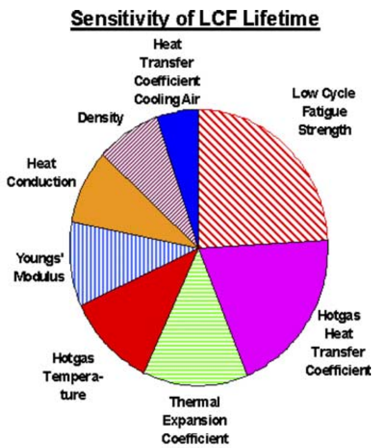

Fig. 6. Cumulative distribution function of the failure modes (left) and sensitivities of the low cycle fatigue failure (right).

usually ignored. The sensitivities shown in Fig. 6 illustrate that the scatter of the SN-curve is indeed the most important influence parameter, but still it is only responsible for one quarter of the effect on the failure probability, with the other input variables together making up for the remaining three quarters.

With a total computation time of 2.5 h per analysis, it would have been impractical to run either the Monte-Carlo simulations or the Design of Experiments in a reasonable time. The analysis runs were performed in parallel in both cases using 35 different computers with different operating systems to reduce the overall wall-clock time.

6.2. Balancing of a compressor blade with uncertainties

The application example illustrates the balancing of a compressor blade, which is an unconstrained optimization problem under uncertainties. The problem is solved using the DesignXplorer in two steps. First the optimization problem is solved deterministically, i.e., by ignoring the uncertainties. Then the probabilistic analysis demonstrates that in real-life, i.e., under the existence of uncertainties, the deterministic solution does not exist.

6.2.1. Description of the deterministic model

The blade geometry is illustrated in Fig. 7. The blade is attached to a disk at the dovetail, which is modeled by fixed boundary conditions. The blade is rotating at 15,000 RPM causing centrifugal loads. As a result the blade shows stress concentrations for the maximum principal stress close to the fillet radius on both sides of the airfoil, as shown in Fig. 7. The tangential and the axial position of the tip of the blade is used as design variable to balance the blade. These two parameters are also referred to as tangential and axial *leaning* denoted with x_{tang}, y_{axial}. The peak values of the maximum principal stress on the pressure and suction side are denoted with σ_{p} and σ_{s}, respectively. The optimization problem reads as follows:

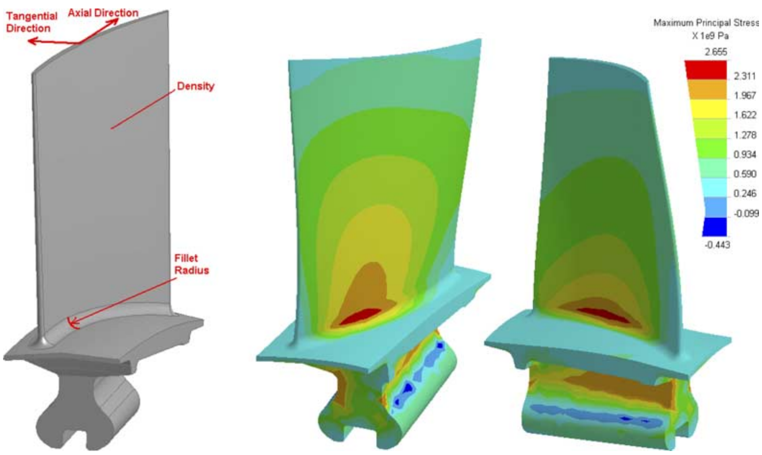

Fig. 7. Compressor blade geometry (left) and stress concentrations for maximum principal stress on suction side (middle) and pressure side (right).

$$\begin{aligned} \text{Minimize}: \quad & \Delta\sigma^2 = (\sigma_p - \sigma_s)^2, \\ \text{For} \quad & 0.65 \leqslant x_{\text{tang}} \leqslant 1.05, \\ & 0.05 \leqslant y_{\text{axial}} \leqslant 0.35. \end{aligned} \tag{15}$$

6.2.2. Deterministic results

If uncertainties are ignored, it can be shown, that the optimization problem in deed has a solution. If the blade tip is positioned too far out in negative tangential direction, then the centrifugal loads will cause a bending moment and bending stresses. An imbalance with opposite sign exists, if the blade tip is positioned too far out in positive tangential direction. Hence, there is a point in between, where the stress peaks are identical and the blade is balanced.

In Fig. 8 ,the response surfaces for the squared stress difference $\Delta\sigma^2$ based on Design of Experiments and Variational Technology are plotted. Overall both methods predict a very similar behaviour. The differences between the two plots can be explained by the accuracies of the two methods. Based on these response surfaces, the deterministic optimization problem was solved and the results are summarized in Table 6. Apparently, the results using the two methods disagree in the location of the optimum point. This is because for both methods the response surfaces resembles is a long stretched valley that is almost flat in longitudinal direction as illustrated in Fig. 8. Hence, only a small disagreement in $\Delta\sigma^2$ between the two response surfaces causes the obvious difference in the optimum point location.

6.2.3. Description of the probabilistic model

For the probabilistic analysis, the design variables are placed at the optimum values obtained by the deterministic optimization using the Variational Technology. It is noted, that if the finite element analysis is executed at the optimum point, the difference between the stress peak on the pressure and suction side is not perfectly zero. To correct the numerical inaccuracy, a modified objective function is defined as $\Delta\sigma^2_{\text{mod}} = (\sigma_p - \sigma_s - \Delta\sigma_{\text{FE}})^2$. Here, $\Delta\sigma_{\text{FE}}$ is the remaining stress dif-

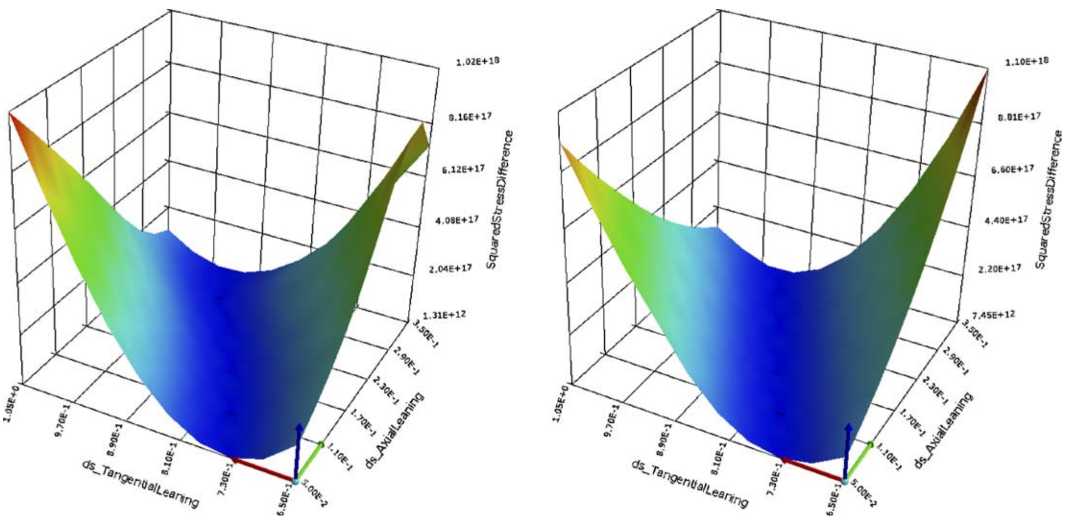

Fig. 8. Response surfaces for $\Delta\sigma^2$ based on Design of Experiments (left) and Variational Technology (right).

Table 6
Deterministic optimization results

Name	Initial value	DOE optimum	VT optimum
x_{tang} (mm)	0.85	0.82800	0.75354
y_{axial} (mm)	0.20	0.18517	0.07056
σ_p (MPa)	1357.6	1224.95	1222.74
σ_s (MPa)	1124.9	1224.95	1222.74
$\Delta\sigma^2$ (MPa^2)	1527164	$2.799\mathrm{e}-2$	$1.627\mathrm{e}-6$
CPU time (s)	89.1	$9 \times 89.1 = 801.9$	216.6

ference from the finite element analysis at the optimum point. At the optimum point $\Delta\sigma^2_{mod}$ is now exactly zero.

There are two random input variables, namely the material density and the fillet radius between the airfoil and the platform, as indicated in Fig. 7. The material density follows a normal distribution with a mean value 4620 and a standard deviation of 161.7. The fillet radius follows a Beta distribution with parameters 1.9 and 1.4 ranging from 0.23 and 0.27.

6.2.4. Probabilistic results

To quantify the scatter of the $\Delta\sigma^2_{mod}$ 100,000 Monte-Carlo simulations were performed on the response surfaces. The resulting cumulative distribution function for $\Delta\sigma^2_{mod}$ is given in Fig. 9. It can be concluded that under the existence of uncertainties the probability of having a perfectly balanced blade is negligibly small, i.e., under real-life conditions uncertainties will always ‘destroy’ the optimum obtained by ignoring uncertainties.

6.3. Robust design of a body-in-white car structure

The application example is a structure with beams and plates, representing a simplified body-in-white frame of a car. The example illustrates how the DesignXplorer can be used to

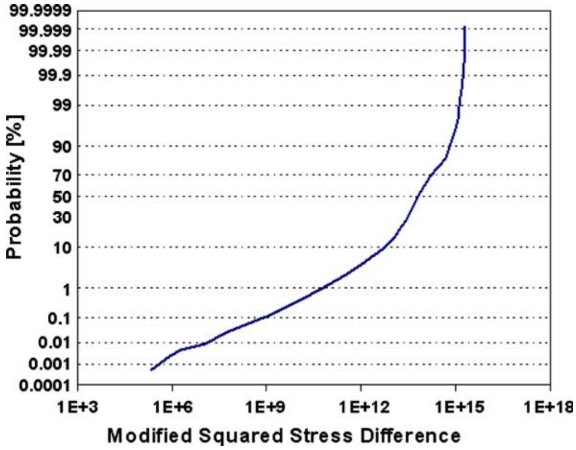

Fig. 9. Cumulative distribution function of $\Delta\sigma^2_{mod}$.

handle multi-objective optimization problems under the existence of uncertainties. To optimize the fuel efficiency, noise emissions and driving comfort of a car structure, several parameters need to be looked at, namely its weight, the stiffness of the frame and the eigenfrequencies of the structure. Optimizing a car not only involves the mere minimization or maximization of those quantities, but it is also necessary that these quantities are not too much affected by uncertainties, which means the optimized design must be robust and reliable. Very often, when multiple goals must be achieved, some of the goals are in conflict with each other. This application example demonstrates, that in real life under the existence of uncertainties, also statistical properties of the result parameters must be included, when looking for such conflicts.

6.3.1. Description of the deterministic model

The car frame is modeled with beam and shell elements. Two types of finite element analyses are performed, namely the torsional stiffness of the frame is quantified with a static analysis using the maximum deflection and a modal analysis is performed to calculate the first 11 eigenfrequencies with the rear and the front of the floor plate being fixed. The boundary conditions for both analyses and the corresponding results are shown in Fig. 10. There are four design variables to optimize the car frame, namely the car length, the car height, the floor width and the roof width. All design variables are geometry parameters defined by a CAD system.

6.3.2. Description of the probabilistic model

There are two random input variables, namely the Young's modulus and the material density. The Young's modulus follows a Gaussian distribution with mean value 200,000 MPa and a standard deviation 10,000 MPa and the material density follows a lognormal distribution with a mean value of 7,850 kg/m^3 and a standard deviation of 392.5 kg/m^3.

6.3.3. Probabilistic results

To quantify the uncertainty of the weight, torsional deflection and the eigenfrequencies, all probabilistic methods discussed above were used. Fig. 11 compares the cumulative distribution

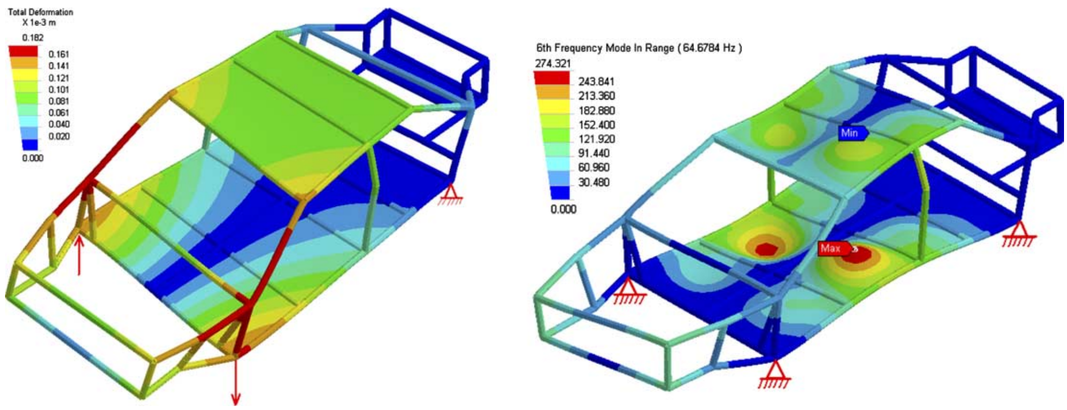

Fig. 10. Torsional deflection (left) and the 6th eigenmode (right) of the car frame.

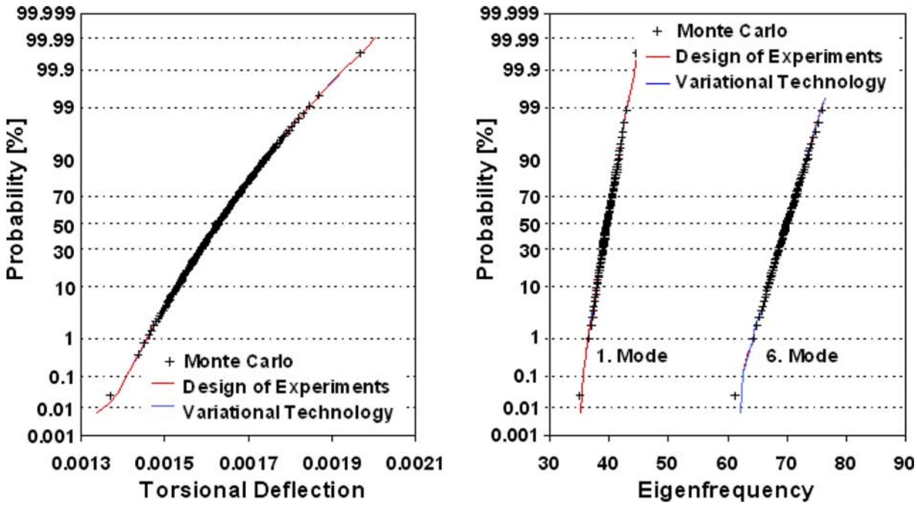

Fig. 11. CDF of torsional deflection (left) and 1st and 6th eigenfrequency (right).

Table 7
Computation time (in seconds) to determine the cumulative distribution functions

Process step	Static analysis			Modal analysis		
	MCS	DOE	VT	MCS	DOE	VT
Building response surfaces	–	312.3	195.9	–	251.1	159.9
Monte-Carlo simulation	347,000	5.0	18.0	279,000	4.0	88.0
Total CPU time	347,000	317.3	213.9	279,000	255.1	247.9

functions obtained from 2'500 Monte-Carlo simulations of the PDS using the finite element model and 10,000 Monte-Carlo simulations using the response surfaces obtained with Design of Experiments and Variational Technology of the DesignXplorer. It is obvious from Fig. 11 that the results for Design of Experiments and Variational Technology are indistinguishably close and match the Monte-Carlo results very well. In Table 7 also the computational effort of the three methods is compared, which illustrates the strength of response surface methods in this case. Particularly, response surfaces based on Variational Technology proved to be highly efficient. The CPU time for the Monte-Carlo simulations in Table 7 includes a factor of 4 to make up for the fact that only 2500 simulations have been performed compared to 10,000 for the other methods.

6.3.4. Robust design study

An optimized car frame shall be given if the weight and the torsional deflection are minimized and all eigenfrequencies are maximized. In addition, to achieve a robust design the standard deviations of all these quantities shall be minimized. Without going into details, it can be stated, that bringing the mean values of the response quantities on target does not lead to a conflict. However,

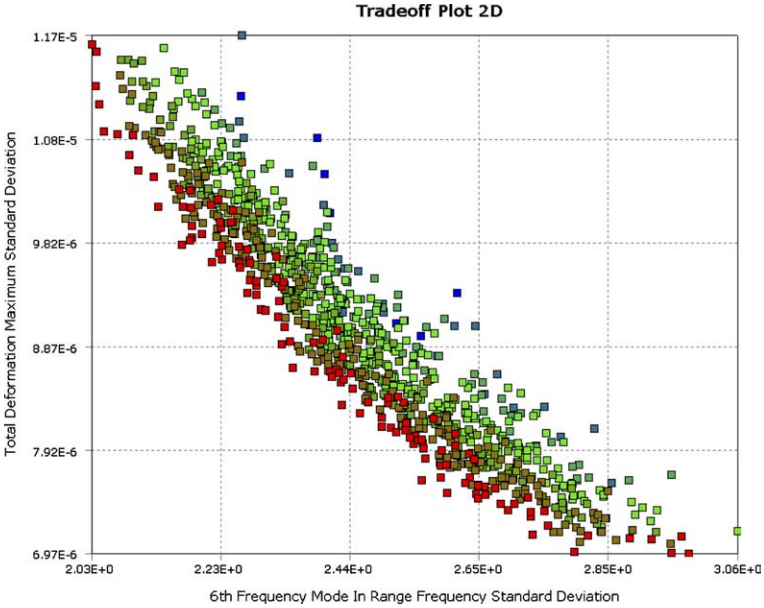

Fig. 12. Trade-off between standard deviations for torsional deflection and 6th eigenfrequency.

minimizing the standard deviations shows conflicts as illustrated in Fig. 12 for the example of the standard deviations of the torsional deflection and the 6th eigenfrequency. Minimizing both standard deviations at the same time is not possible. This situation is a trade-off scenario, where improving one goal can only be done at the expense of another. An informed decision of how far the conflicting goals can be achieved or must be sacrificed, is only possible if the trade-off is quantified and visualized like in Fig. 12.

7. Summary

The current paper outlines, explains and compares the capabilities of the ANSYS Probabilistic Design System and the ANSYS DesignXplorer. The probabilistic methods implemented in these tools are discussed and the advantages and disadvantages are compared. The theoretical background of these methods and their accuracy is given special attention. A special topic in this context is the Variational Technology, which provides high order response surfaces based on a single finite element analysis. Three application examples are used to illustrate the capabilities of the tools.

References

[1] Formica A. A science based multiscale approach to engineering stochastic simulations. In: Marczyk J, editor. Computational stochastic mechanics in a meta-computing perspective. Barcelona, Spain: CIMNE; 1997.

[2] Taguchi G, Konishi S. Taguchi methods: signal-to-noise ratio for quality evaluation. Quality engineering series, vol. 3. (Burr Ridge, IL): Irwin Professional Publishing; 1993.

[3] Montgomery DC. Design and analysis of experiments. (New York, NY): Wiley; 1991.

[4] Parks JM. On stochastic optimization: Taguchi methods™ demystified; its limitations and fallacy clarified. Probab Eng Mech 2001;16(1):87–101.

[5] Shannon CE. A mathematical theory of communication. Bell Syst Tech J 1948;27(7,10):379–423. 623–656.

[6] Harry MJ, Lawson JR. Six Sigma producibility analysis and process characterization. (Boston, MA): Addison-Wesley; 1992.

[7] Ang AH-S, Tang WH. Probabilistic concepts in engineering planing and design. Decision, risk and reliability, vol. II. (New York, NY): Wiley; 1984.

[8] Liu P-L, Der Kiureghian A. Multivariate distribution models with prescribed marginals and covariances. Probab Eng Meth 1986;1(2):105–12.

[9] Craney TA. Response surface methodology developments for probabilistic engineering design. Master's thesis. (College Park, MD): University of Maryland; 2002.

[10] Hammersley JM, Handscomb DC. Monte Carlo methods. London: Chapman & Hall; 1964.

[11] Press WH, Teukolsky SA, Vetterling WT, Flannery BP. Numerical recipes in C – the art of scientific computing. 2nd ed.. London: Cambridge University Press; 1992.

[12] Mastumoto M, Nishimura T. Mersenne twister: A 623-dimensionally equidistributed uniform pseudorandom number generator. ACM Trans Modell Comput Simul 1998;8:3–30.

[13] Kececioglu D. Reliability engineering handbook, vol. 2. (Upper Sadle River 07458, NJ): Prentice-Hall; 1991.

[14] Ayyub BM, Lai K-L. Structural reliability assessment using latin hypercube sampling. In: Ang AH-S, Shinozuka M, Schuëller G, editors. Proceedings of the 5th international conference on structural safety and reliability (ICOSSAR). (San Francisco, CA): American Society of Civil Engineers; 1989. p. 1177–84.

[15] Florian A. An efficient sampling scheme: updated latin hypercube sampling. Probab Eng Mech 1992;7:123–30.

[16] Ang AH-S, Tang WH. Probabilistic concepts in engineering planing and design. Basic principles, vol. I. (New York, NY): Wiley; 1975.

[17] Myers RH, Montgomery DC. Response surface methodology. 2nd ed.. (New York, NY): Wiley; 2002.

[18] Box GEP, Behnken DW. Some new three level designs for the study of quantitative variables. Technometrics 1960;2(4):455–76.

[19] Neter J, Kutner MH, Nachtsheim CJ, Wasserman W. Applied linear statistical models. 3rd ed.. (Boston, MA): McGraw-Hill; 1996.

[20] Box GEP, Cox DR. An analysis of transformation. J R Statist Soc Ser B 1964(26):211–43.

[21] Yeo I-K, Johnson RA. A new family of power transformations to improve normality or symmetry. Biometrica 2000;87(4):954–9.

[22] Haftka R. Second-order sensitivity derivatives in structural analysis. AIAA J 1982;20:1765–6.

[23] Guillaume P. Dérivées d'ordre supérieur en conception optimale de formes; 1994.

[24] Beley J, Broudiscou C, Guillaume P, Masmoudi M, Thevenon F. Application de la méthode des dérivées d'ordre élevé a l'optimisation de structures. Rev europ éléments finis 1996;5(5–6):537–67.

[25] Oppelstrup J. ESPRIT HPCN PST activity OPTIBLADE: Fan blade shape optimization by parametric CFD, Public final report, HPCN TTN Network. Stockholm, Sweden: Center for Parallel Computers, Royal Institute of Technology; 1999.

[26] Thevenon F, Rochette M, Izabelle A, Girard P, Colombani D. Paramétrisation d'un logiciel de calcul électromagnétique non linéaire par dérivTés d'ordre élevé. In Proceedings of NUMELEC; 1997. p. 44–5.

[27] Rogers L. Derivatives of eigenvalues and eigenvectors. AIAA J. 1970;8(5):943–4.

[28] Nelson R. Simplified calculation of eigenvectors derivatives. AIAA J. 1976;14:1201–5.

[29] Ojalvo I. Efficient computation of mode-shape derivatives for large dynamic systems. AIAA J 1987;25(10):1386–90.

[30] Guillaume P, Huard A. Multivariate Padé approximation. J Comput Appl Math 2000;121:197–219.

[31] Reh S, Scheu M. Sensitivity controlled response surface approach for reliability based design. In Proceedings of the 41th international gas turbine and aeroengine congress & exhibition, No. ASME 96-GT-268, Birmingham, UK; 1996.

[32] Reh S, Palfi T, Nemeth NN. Probabilistic analysis techniques applied to lifetime reliability estimation of ceramics. In Proceedings of JANNAF interagency propulsion conference on advanced materials and safe life, Colorado Springs, CO; 2003.